Crystalline niobia with tailored porosity as support for cobalt catalysts for the Fischer–Tropsch synthesis

C. Hernández Mejía, J.H. den Otter, J.L. Weber, K.P. de Jong*

Inorganic Chemistry and Catalysis, Debye Institute for Nanomaterials Science, Utrecht University, Universiteitsweg 99, 3584 CG Utrecht, The Netherlands

ARTICLE INFO

ABSTRACT

Structure and catalytic performance of niobia-supported cobalt catalysts were studied based on crystal phase, porosity and cobalt loading. Crystalline niobia as support proved to be a prerequisite to obtain highly active and selective Co/niobia Fischer–Tropsch catalysts, whereas amorphous niobia showed minimal activity. Crystallization changed the porous morphology of $Nb_2O_5 \cdot nH_2O$ resulting in a dense material with low specific pore volume and specific surface area. Multiple impregnations on crystalline Nb_2O_5 were necessary to achieve cobalt loadings higher than 6 wt.%; this led to larger cobalt particles, diminished interaction of cobalt with niobia and therefore decreased activity per unit weight of cobalt and C_{5+} selectivity. Carbon deposition via sucrose pyrolysis was employed in order to partly maintain the porosity during crystallization. The obtained porous crystalline niobia was used as support for cobalt catalysts with higher metal loadings. STEM-EDX mapping characterization of the catalysts provided unique information for this kind of materials, e.g. cobalt distribution and particle size. The catalysts showed high cobalt-normalized catalytic activity and C_{5+} selectivity for the Fischer–Tropsch synthesis under industrially relevant conditions. Moreover, higher cobalt loadings led to an increased catalyst-weight normalized catalytic activity.

1. Introduction

Fischer–Tropsch synthesis involves the transformation of synthesis gas (a mixture of H_2 and CO) to chemicals and ultra-clean fuels. Particularly, cobalt-based catalysts are industrially relevant for the production of long-chain hydrocarbons (C_{5+}). These catalysts offer high selectivity, activity and stability, especially when promoted with noble metals and/or transition metal oxides [1]. Since the first reports by Schmal et al. [2–4], cobalt supported on niobia (Nb_2O_5) has gained considerable interest due to its notably high selectivity towards C_{5+}. Furthermore, the Co/Nb_2O_5 system shows great activity per unit weight of cobalt and markedly increases turnover frequencies upon noble metal promotion [5–8].

Niobia as support has been reported to be effective for cobalt Fischer–Tropsch catalysts solely in the crystalline form. Generally, this crystalline niobia has a very low specific pore structure compared to typical Fischer–Tropsch supports (e.g. SiO_2 and γ-Al_2O_3), limiting the application of high metal loadings. Therefore, crystalline niobia with higher porosity would allow higher cobalt loadings and dispersion. Several methods have been reported for the synthesis of porous Nb_2O_5 [9]. However, despite the higher porosity obtained, most of these methods have basic disadvantages to be applied in large-scale support

synthesis. Expensive and highly reactive precursors were involved (e.g. $NbCl_5$, $Nb(OEt)_5$, copolymers) [10–12] or the resulting Nb_2O_5 had low crystallinity and high acidity [13–15]. In order to be used as Fischer–Tropsch support material, where large quantities are necessary, a simple and efficient method is required. Contrary to the common Nb_2O_5 crystalline form, amorphous niobium oxide hydrate ($Nb_2O_5 \cdot nH_2O$) has a mesoporous structure with relatively high specific pore volume and specific surface area. However, due to its acidic properties, niobium oxide hydrate is reactive towards cobalt salts during catalyst preparation, leading to formation of inactive species for Fischer–Tropsch synthesis. Niobium oxide hydrate can be effectively used as precursor for niobia via thermal crystallization at temperatures greater than 500 °C as has been shown by Schmal and co-workers [2–4]. This thermal treatment however decreases considerably porosity and specific surface area.

Here we report the influence of niobia crystal phase, porosity and cobalt loading on the catalysts' structure and performance in Fischer–Tropsch synthesis. Sucrose impregnation, polymerization and pyrolysis over the niobium oxide hydrate surface was employed in order to maintain the porosity during crystallization. This facile method resulted in a crystalline niobia material which preserved a great fraction of the mesoporous structure of the niobium oxide hydrate. The

material was used as support to prepare cobalt catalysts and tested for the Fischer–Tropsch synthesis. These catalysts showed high cobalt-specific catalytic activity and good C_{5+} selectivity, furthermore due to the higher cobalt loading the catalyst weight-based activity was markedly higher.

2. Experimental

2.1. Catalyst preparation

Niobium oxide hydrate ($Nb_2O_5 \cdot nH_2O$, HY-340, AD/4465) was obtained from Companhia Brasileira de Metalurgia e Mineração − CBMM. Thermal treatment of niobium oxide hydrate was performed in stagnant air, air flow or N_2 flow.

Mesoporous crystalline niobia (Nb_2O_5-MC): The support was prepared starting from niobium oxide hydrate ($Nb_2O_5 \cdot nH_2O$, HY-340, AD/4465, 75–150 μm), which was firstly dried under dynamic vacuum. Thereafter it was impregnated with a sucrose aqueous solution (0.25 g cm^{-3}), using equal amounts of sucrose and $Nb_2O_5 \cdot nH_2O$ (m/m).

In order to polymerize and pyrolize the sucrose, the impregnated niobium oxide hydrate was heated in a tubular furnace under N_2 flow at 150 °C for 2 h (5 °C min^{-1}). The sample was then heated to 600 °C for 2 h (20 °C min^{-1}) under N_2 flow. The obtained sample, a black uniform powder, was left to cool down to room temperature. Finally, the carbon was burned off at 400 °C for 4 h (5 °C min^{-1}) in 30 vol.% O_2/N_2 flow.

The cobalt catalysts were prepared using incipient wetness impregnation of niobium oxide hydrate calcined at temperatures between 120 °C and 600 °C or Nb_2O_5-MC. Prior to impregnation the supports (75–150 μm grains) were dried under vacuum at 80 °C for 1 h. The impregnation was performed with aqueous solution of $Co(NO_3)_2 \cdot 6H_2O$ (Acros, 99%), where the concentration depended on the pore volume of the support used and the target metal loading. Multiple impregnations were necessary to achieve Co loadings larger than 6 wt.% for niobia with low specific pore volume. In the next step, the catalysts were dried for 12 h at 60 °C in stagnant air and subsequently calcined for 2 h at 350 °C (3 °C min^{-1}) in a fixed bed reactor under N_2 flow. Metal loadings were defined as the mass of metallic cobalt per gram of reduced catalyst.

2.2. Characterization

Powder X-ray diffractograms were measured using a Bruker-AXS D2 Phaser X-ray diffractometer, Co-Kα radiation (λ = 1.789 Å). For calcined catalysts Co_3O_4 crystallite size was calculated using the Scherrer equation (k = 0.9) to the (311) diffraction line at 2θ = 43.0° or (220) diffraction line at 2θ = 36.5°. *In situ* XRD was measured using a Bruker-AXS D8 Advance X-ray diffractometer, Co-Kα radiation (λ = 1.789 Å). The sample was heated to 350 °C (2 h, 5 °C min^{-1}) in 25 vol% H_2/He. A micromeritics TriStar 3000 apparatus was used to perform N_2-physisorption at −196 °C. Prior to analysis the sample was dried at either at 120 or 200 °C for 16 h in N_2 flow. Specific surface area was calculated using the BET theory for p/p$_0$ = 0.06–0.25. The pore size distribution was determined using the BJH theory applied to the adsorption branch. The specific mesopore volume was calculated using single point at p/p$_0$ = 0.98. Thermogravimetric analysis was performed using a TGA Q50 equipment, around 20 mg of sample were placed in a platinum crucible under 60 cm^3 min^{-1} air flow and heated until 400 °C (15 °C min^{-1}) for 4 h thereafter heated until 1000 °C (15 °C min^{-1}), 40 cm^3 min^{-1} N_2 flow was used as reference. Temperature programmed reduction (TPR) analyses were performed using a Micromeritics Autochem 2990 instrument, where 100 mg sample were dried at 120 °C for 1 h in Ar flow followed by reduction from room temperature up to 1000 °C (10 °C min^{-1}) in a 5 vol% H_2/Ar flow. Bright field transmission electron microscopy (TEM) imaging was performed using a Tecnai 12 operated at 120 kV. Scanning transmission electron microscopy (STEM-EDX) images were acquired with a Philips
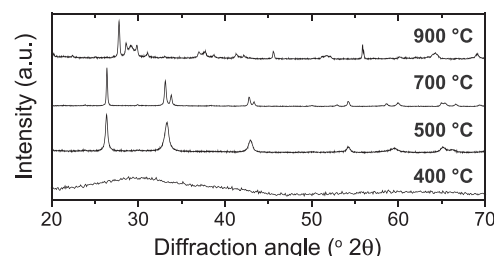

Fig. 1. X-ray diffractograms for Niobium oxide hydrate calcined in stagnant air at 400, 500, 700 and 900 °C.
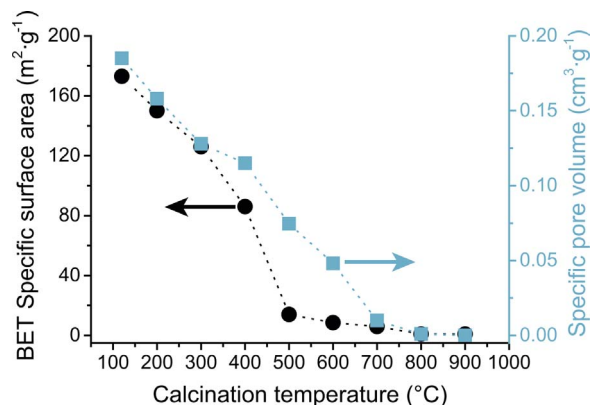

Fig. 2. Decrease in specific surface area (black circles) and specific pore volume (blue squares) of niobium oxide hydrate upon temperature increase.

Tecnai-20 FEG (200 kV) microscope equipped with an energy dispersive X-ray (EDX) and high-angle annular dark-field (HAADF) detector.

2.3. Catalytic testing

Low pressure catalytic testing was performed in a quartz glass plug-flow reactor, typically loaded with 15–20 mg catalyst (38–150 μm) diluted with 200 mg SiC. Typically, the catalysts were reduced in situ at 350 °C (5 °C min^{-1}, 2 h) in a 20/40 mL min^{-1} H_2/Ar flow. Fischer-Tropsch catalysis was performed at 220 °C, 1 bar, H_2/CO = 2.0 v/v, GHSV = 24000–48000 h^{-1}, CO conversion < 5%. C_1–C_{18} products were analyzed by online gas chromatography (Varian 430 GC, CP sil-5 column). Activity and selectivities were reported after at least 40 h on stream. High pressure catalytic testing was performed using an Avantium Flowrence 16 parallel, continuous flow, fixed bed reactor system. Typically, 100 mg catalyst (38–150 μm) were diluted with 300 mg SiC and loaded in a stainless-steel reactor. The catalysts were reduced in situ at atmospheric pressure in a 25 vol% H_2/He flow, for 8 h at 350 °C (heating rate of 1 °C min^{-1}). Thereafter, reactors were cooled down to 180 °C and the gas stream was switched to synthesis gas, H_2/CO = 2.0 v/v, GHSV 4500 h^{-1}. Reactors were pressurized to 20 bar and subsequently heated to reaction temperature 220 °C (1 °C min^{-1}), CO conversion was maintained at 15–25%. Products up to C_9 were analyzed using online gas chromatography. GHSV was defined as total gas flow divided by the catalyst volume.

3. Results and discussion

3.1. Niobium oxide hydrate thermal treatment

Niobium oxide hydrate was characterized by powder X-ray diffraction (XRD) and N_2-physisorption after the different thermal treatments. Niobium oxide hydrate remained amorphous after stagnant air calcination in a muffle oven up to 400 °C (Fig. 1). Crystallization started after calcination at 500 °C, transforming the material into low-
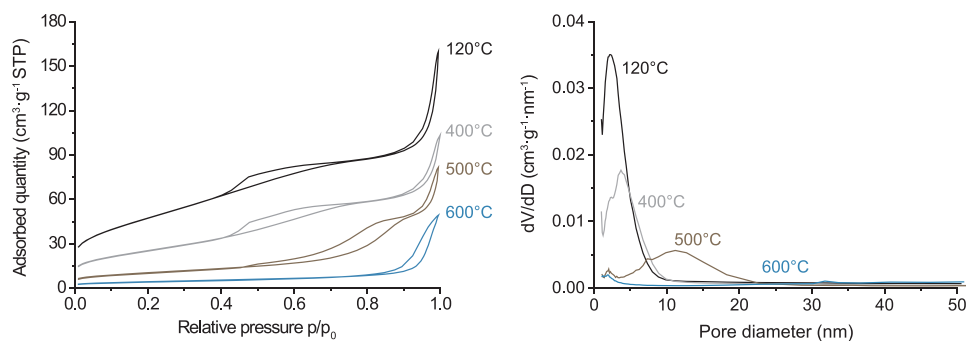
Table 1
Summary of the characterization results for niobia after the different treatments. SA$_{BET}$: specific surface area, PV: specific mesopore volume and PD: pore diameter.

| Crystallization conditions	Crystal phase	SA$_{BET}$ (m^2 g^{-1})	PV (cm^3 g^{-1})	PD (nm)
Niobium oxide hydrate thermal treatment				
120 °C, stagnant air muffle oven	amorphous	173	0.19	2–5
400 °C, muffle oven	amorphous	86	0.12	2–7
600 °C, stagnant air, muffle oven	Pseudo-hexagonal TT	9	0.05	> 50
700 °C, stagnant air, muffle oven	Hexagonal T	6	0.01	> 50
900 °C, stagnant air, muffle oven	Monoclinic H	1	< 0.01	> 50
Modified niobia crystallization				
600 °C, stagnant air, quartz reactor	Pseudo-hexagonal TT	25	0.11	5–60
600 °C, air flow, quartz reactor	Pseudo-hexagonal TT	22	0.06	5–25
600 °C, N$_2$ flow, quartz reactor	Pseudo-hexagonal TT	22	0.06	5–25
Nb$_2$O$_5$–MC	Pseudo-hexagonal TT	56	0.16	2–12
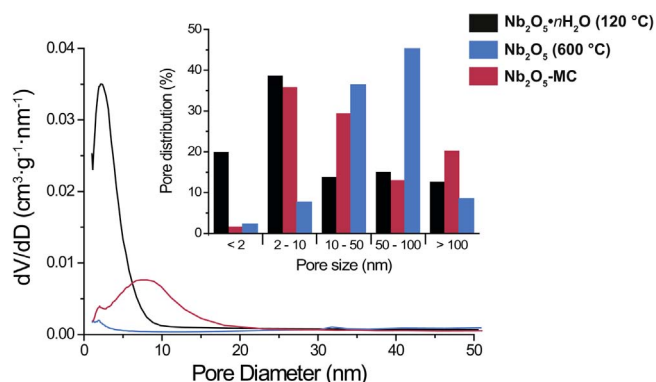
Fig. 4. Pore size distribution for the initial material (niobium oxide hydrate, black) and the crystalline materials: Nb$_2$O$_5$ calcined at 600 °C (blue) and Nb$_2$O$_5$–MC (red). (For interpretation of the references to colour in this figure legend, the reader is referred to the web version of this article.)

crystalline pseudo-hexagonal Nb$_2$O$_5$ TT-phase. Calcination at temperatures above 600 °C led to the orthorhombic Nb$_2$O$_5$ T-phase, as indicated by the splitting of the peaks at 2θ = 33° and 42° · Monoclinic Nb$_2$O$_5$ phase was observed after calcination at 900 °C [16–18].

Increase in calcination temperature changed as well the niobia morphology (Fig. 2). Niobium oxide hydrate after drying at 120 °C had a BET specific surface area and specific mesopore volume of 173 m^2 g^{-1} and 0.19 cm^3 g^{-1} respectively, as determined by N$_2$-physisorption. Upon increasing calcination temperature these values decreased. In particular, after crystallization at 600 °C the specific surface dropped to 9 m^2 g^{-1} and the specific mesopore volume to 0.05 cm^3 g^{-1}.

The porosity of niobium oxide hydrate after drying at 120 °C consisted mainly of 2–5 nm mesopores as indicated by the hysteresis at p/p$_0$ = 0.4–0.7 (Fig. 3) and TEM images (Fig. S1), these mesopores were maintained up to 400 °C. After crystallization at 600 °C most of the mesopores had collapsed and only hysteresis at p/p$_0$ = 0.9 was observed, indicative for larger pores (> 50 nm). These macropores originated from the Nb$_2$O$_5$ interparticle space. Table 1 summarizes the characterization results for the different materials.
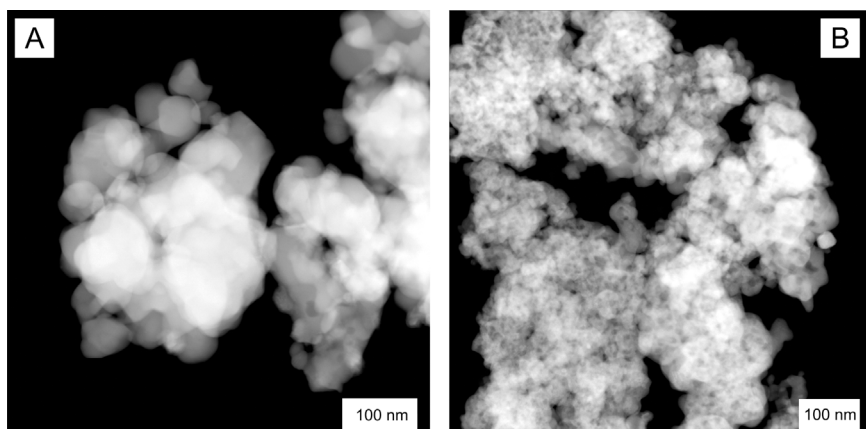

Fig. 5. Dark field STEM images of the crystalline materials: (A) dense Nb$_2$O$_5$ obtained by calcination at 600 °C and (B) porous Nb$_2$O$_5$–MC obtained by sucrose impregnation, pyrolysis and calcination.
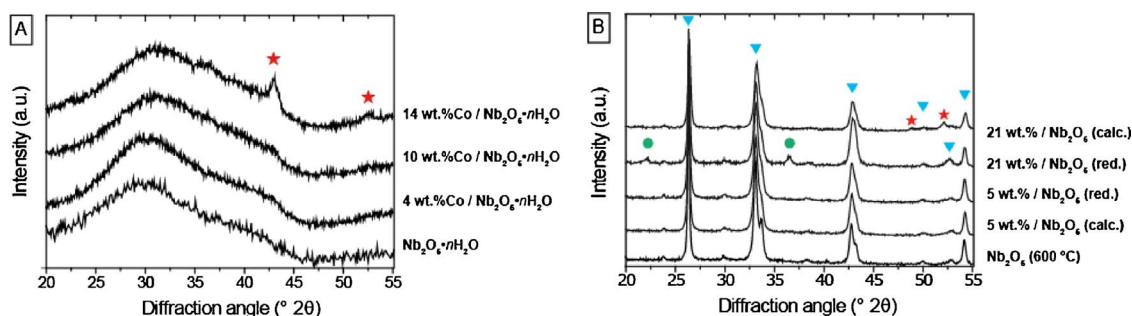
Fig. 6. X-ray diffractograms of the calcined cobalt catalysts supported on amorphous niobium oxide hydrate (A) or crystalline niobia pretreated at 600 °C (B). ★ indicate Co_3O_4, ▼ indicate Nb_2O_5 (T-phase) and ● indicate Co^0.
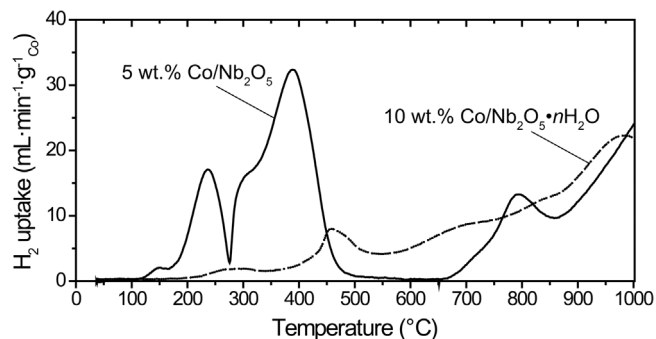

Fig. 7. Temperature programmed reduction profiles for two catalysts after impregnation, drying and calcination: 5 wt.% cobalt supported on crystalline niobia (treated at 600 °C) and 10 wt.% cobalt supported on amorphous niobium oxide hydrate (treated at 120 °C).

3.2. Modified niobia crystallization

Stagnant air, air flow or N_2 flow were used during niobia crystallization at 600 °C to study the effect of different gas atmospheres and hydrodynamics. For all cases, pseudo-hexagonal niobia TT-phase was obtained with BET specific surface areas of 22–25 $m^2 g^{-1}$ (Table 1). Calcination in stagnant air led to a higher specific mesopore volume (0.11 $cm^3 g^{-1}$) than after calcination in N_2 or air flow (0.06 $cm^3 g^{-1}$).

In order to inhibit porosity loss during crystallization, the niobium oxide hydrate pores were filled with sucrose as carbon precursor prior thermal treatment. Niobium oxide hydrate was impregnated with a sucrose solution, which polymerized by the acidic properties of the oxide and thermal treatment at 150 °C. After pyrolysis and crystallization at 600 °C, the obtained black powder showed the pseudo-hexagonal Nb_2O_5 TT-phase (Fig. S2) and a decrease in specific mesopore volume (0.08 $cm^3 g^{-1}$) which might indicate a blockage of the niobia pores by carbon. Thermogravimetric analysis (TGA) in air of this material shows most of the weight loss after 4 h at 400 °C (Fig. S3), indicating that carbon can be effectively removed under these conditions. After carbon was burned off the obtained crystalline material has a mesopore volume of 0.16 $cm^3 g^{-1}$ with a specific surface area of 56 $m^2 g^{-1}$. Fig. 4 shows the pore size distribution of niobium oxide hydrate dried at 120 °C, crystallized at 600 °C and the mesoporous crystalline niobia (Nb_2O_5–MC). Despite the template used not all of the mesopores from niobium oxide hydrate could be maintained during the treatment; however their collapse was retarded compared to normal crystallization at 600 °C. Dark field STEM images of these two crystalline materials are shown in Fig. 5. Clearly the niobia crystallized at 600 °C without template has a dense structure whereas for Nb_2O_5–MC a more porous structure is observed.

3.3. Cobalt deposition

Deposition of cobalt on the support was performed by incipient wetness impregnation method. Niobium oxide hydrate calcined at 120 °C or 600 °C was used as support and deposition of cobalt was performed by single or multiple impregnation (4–21 Co wt.%) followed by drying and calcination at 350 °C. XRD showed no crystalline cobalt species up to 10 wt.% independently of the support used, i.e. amorphous or crystalline niobia. Co_3O_4 was observed only on the calcined samples with > 13 wt.% Co (Fig. 6). Furthermore, samples supported on crystalline niobia were reduced in situ (25 vol.% H_2/He, 350 °C) and still no cobalt species were observed for the low loadings (Fig. 6B). This indicates that for low cobalt loadings poorly crystalline cobalt species, very small crystallite sizes or Co-Nb oxide species were formed independently of the niobia pretreatment, in line with previous reports [19].

The support used, amorphous or crystalline niobia, had a strong impact on the reduction of the cobalt species as shown by the temperature programmed reduction profiles (Fig. 7). The reduction on crystalline niobia proceeded in two steps as previously reported: from Co_3O_4 to CoO and from CoO to metallic Co [19–21]. The reduction temperature is significantly lower if compared with γ-alumina- or silica-supported cobalt catalysts, therefore reduction can be effectively performed at temperatures lower than 400 °C without noble metal promotion. In contrast, cobalt supported on amorphous $Nb_2O_5 \cdot nH_2O$ showed no distinctive reduction peaks until temperatures greater than 450 °C (Fig. 7). A continuous H_2 consumption is observed throughout temperature increase, attributed to reduction of the support. This different reduction profile can be attributed to a stronger interaction between cobalt and niobium oxide hydrate. Most likely no Co_3O_4 was formed after impregnation and calcination but rather Co-Nb oxide species which cannot be easily reduced.

The mesoporous crystalline niobia (Nb_2O_5-MC) was used as support for 6 and 10 wt.% Co, prepared by incipient wetness impregnation. Due to the larger specific pore volume of Nb_2O_5–MC, a higher metal loading could be achieved in a single impregnation step. In general, characterization of niobia-supported catalysts using TEM in the dark or bright field has the challenge of phase distinction between Co_3O_4 and Nb_2O_5 due to their similar electron density. Therefore, electron microscopy combined with EDX mapping is an important and powerful technique for the characterization of this kind of materials. Fig. 8 shows the STEM-EDX mapping images of the Nb_2O_5–MC-supported catalysts and for comparison purposes a 6 wt.% Co supported on pretreated Nb_2O_5 at 600 °C. STEM-EDX mapping images were taken after reduction at 350 °C and passivation. A comparison of the Nb_2O_5–MC-supported catalysts (Fig. 4A, B) shows that the 6 wt.% Co catalyst had smaller particles (9.7 ± 3.3) than the 10 wt.% Co (13.9 ± 6.5), which is expected for higher metal loadings. Still these two catalysts show a smaller particle size if compared to the one supported on the dense niobia calcined at 600 °C (15.6 ± 4.3, Fig. 4C). The porous morphology of Nb_2O_5–MC is suggested to restrict particle growth during reduction.
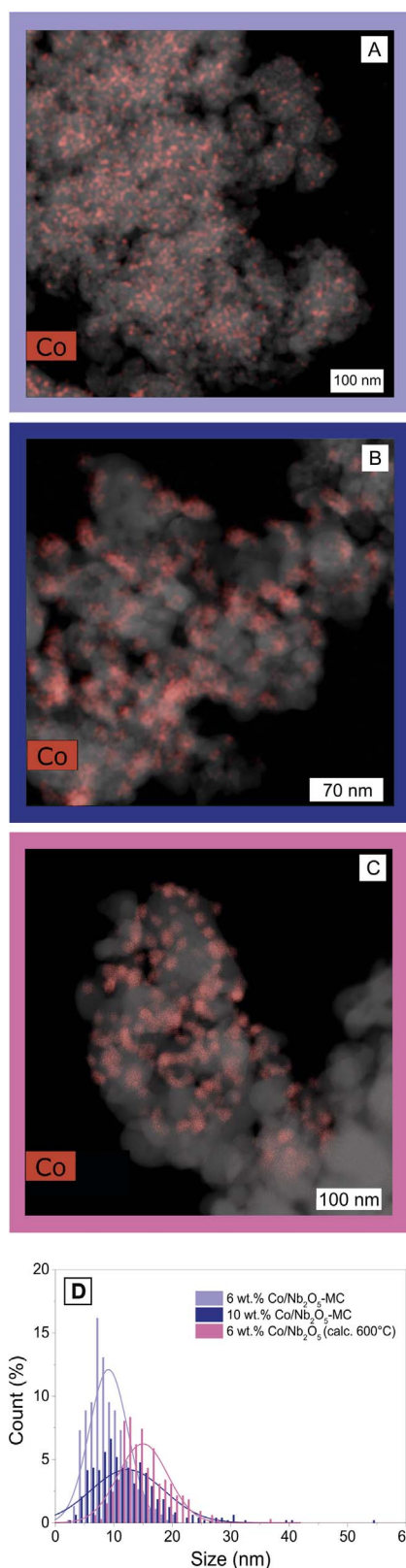
Fig. 8. STEM-EDX mapping images of cobalt catalysts after reduction and passivation, cobalt is shown in red and the support in grey. Nb_2O_5–MC supported catalysts with 6 wt.% Co (A) and 10 wt.% Co (B). 6 wt.% Co catalyst supported on niobia pretreated at 600 °C (C). Histogram from the particle size measurement (D). (For interpretation of the references to colour in this figure legend, the reader is referred to the web version of this article.)

Table 2
Summary of the catalytic results for the Fischer–Tropsch reaction at 1 or 20 bar, 220 °C and $H_2/CO = 2$.

Support[a]	Number of impregnations	Co loading (wt.%)	Cobalt-Time-Yield[b] $(10^{-5}$ $mol_{CO}g_{Co}^{-1}s^{-1})$	C_{5+} selectivity (wt.%)
Amorphous $Nb_2O_5 \cdot nH_2O$ (120 °C)	2	10	< 0.3	45
Amorphous $Nb_2O_5 \cdot nH_2O$ (400 °C)	1	5	0.5	49
Crystalline Nb_2O_5 (600 °C)	1	5	3.0	70
	2	10	2.5	64
	3	15	2.2	60
	4	17	1.5	55
	4	21	2.1	42
	1	6	4.5 (20 bar)	80 (20 bar)
Nb_2O_5–MC	1	6	4.2 (20 bar)	80 (20 bar)
			2.1 (1 bar)	64 (1 bar)
	1	10	3.7 (20 bar)	81 (20 bar)
			2.0 (1 bar)	65 (1 bar)

[a] In brackets the calcination temperature of the support.
[b] Catalysts tested at 20 bar are indicated and the value reported is after 100 h TOS, if not indicated catalysts were tested at 1 bar, 40 h TOS.
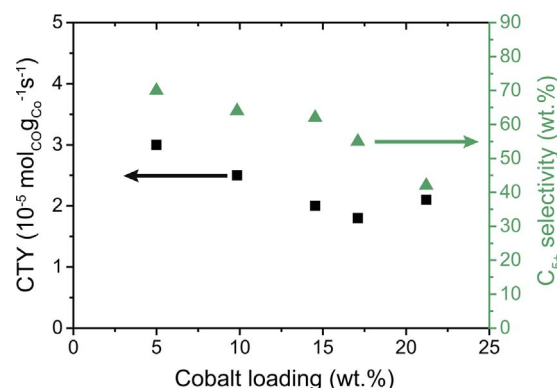

Fig. 9. Cobalt-weight normalized activity (CTY) and C_{5+} selectivity for the Fischer–Tropsch reaction (1 bar, 220 °C and $H_2/CO = 2$). Cobalt was deposited by multiple impregnations (loadings ≥ 10 wt.%) on crystalline niobia pretreated at 600 °C.

3.4. Catalytic testing

Prepared catalysts were investigated for the Fischer–Tropsch reaction at 1 bar, 220 °C and $H_2/CO = 2$ to obtain activity and selectivity data (Table 2). 5 wt.% Co supported on crystalline niobia (pretreated at 600 °C) was reduced prior to reaction conditions at 350 °C, cobalt-weight normalized activity (Cobalt-Time-Yield: 3×10^{-5} $mol_{CO}g_{Co}^{-1}s^{-1}$) and C_{5+} selectivity (~ 70 wt.%) were observed after 40 h on stream similar to results observed previously for promoted Co/SiO_2 catalysts [22]. Reduction at 500 °C prior to reaction led to 10 times decrease in CTY. Since niobia is a reducible support, SMSI effects by reducing at higher temperatures are expected and have been observed previously by Silva et al. [3]. Catalysts supported on amorphous niobium oxide hydrate showed low catalytic activity (Table 2), this might be due to formation of irreducible cobalt species on this support as shown by TPR. Encapsulation of cobalt in the mesopores (2–5 nm) of this material during catalyst preparation or catalytic testing might have also led to inaccessibility of the active sites. The amorphous form of niobia appears too reactive thereby inhibiting activation of cobalt for the Fischer–Tropsch reaction and thus crystalline niobia is required to obtain active cobalt catalysts.

Catalysts prepared by multiple impregnations showed a decrease in CTY and C_{5+} selectivity by increasing the cobalt loading (Fig. 9). Considering the low specific surface area of the support, small interparticle distance at higher cobalt loadings can lead to particle growth
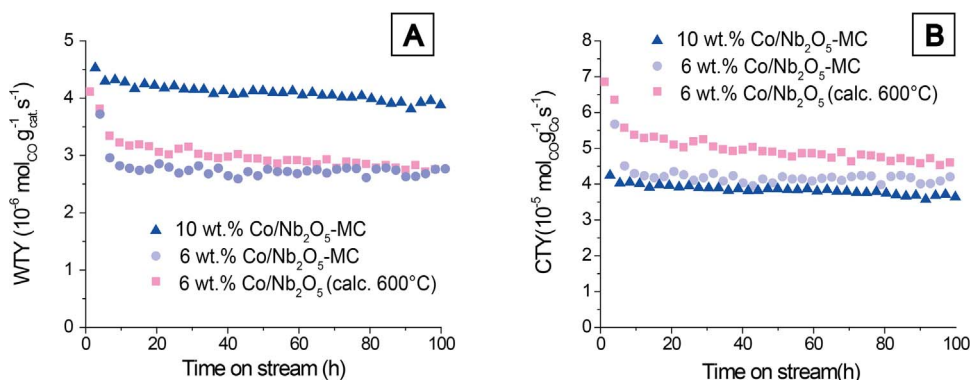
Fig. 10. Catalytic activity up to 100 h on stream for Co supported on crystalline niobia. (A) Activity normalized per catalyst weight (Weight Time Yield, WTY) and (B) activity per unit weight of cobalt (Cobalt Time Yield, CTY).

and sintering. In a similar way, larger particles lead to a decreased Co-Nb_2O_5 interface, where the chain growth probability is larger, therefore decreasing the C_{5+} selectivity [5].

Nb_2O_5–MC supported catalysts were tested both at 1 and at 20 bar, 220 °C and $H_2/CO = 2$. Results are shown on Table 2. For comparison purposes, a 6 wt.% cobalt catalyst with niobia treated at 600 °C as support was also tested at high pressure. The catalytic activity normalized per catalyst weight (Weight Time Yield, WTY) tested at 20 bar is shown in Fig. 10A. Clearly the 10 wt.% Co/Nb_2O_5–MC catalyst (blue triangles) outperforms the 6 wt.% Co catalysts because of the higher metal content. The 6 wt.% Co/Nb_2O_5–MC catalyst (purple circles) shows a slightly lower WTY than the 6 wt.% Co/Nb_2O_5 (pretreated at 600 °C, pink squares) at the initial hours of the experiment, however after 70 h on stream its steady deactivation leads to the same activity as the Nb_2O_5–MC supported catalyst. Fig. 10B shows the CTY, the three catalysts reach virtually the same value after 100 h on stream. The catalyst supported on Nb_2O_5 treated at 600 °C shows a more pronounced deactivation throughout time compared with the Nb_2O_5–MC supported catalysts. One of the main causes of deactivation for cobalt Fischer–Tropsch catalysts is particle sintering. It is possible to think that the porous structure of the Nb_2O_5–MC support has retarded the cobalt particles from sintering, leading to more stable catalysts during long time on stream. In contrast, the flat surface of Nb_2O_5 treated at 600 °C allows particle growth and decrease in catalytic activity with time. The three catalysts showed a similar C_{5+} selectivity of ~80 % during the catalytic experiments (Table S1).

4. Conclusions

The pore structure of amorphous niobium oxide hydrate was determined to be intricate with 2–5 nm mesopores giving rise to high specific surface and pore volume. Collapse of this pore structure during thermal treatment led to a drastic decrease in specific surface area and specific mesopore volume. For the synthesis of active cobalt Fischer–Tropsch catalysts, niobia crystallization at temperatures above 400 °C prior to cobalt deposition was found necessary to allow formation of reducible cobalt oxide species. Consequently, no activity was observed for the Fischer–Tropsch synthesis using amorphous niobia as support. Contrastingly, cobalt supported on crystalline niobia prepared by impregnation and reduced at 350 °C prior reaction conditions showed remarkably high activity per unit weight of cobalt and C_{5+} selectivity, previously only observed for promoted Co catalysts. Higher reduction temperature (500 °C) significantly decreased the catalyst activity, probably due to coverage of the cobalt surface sites due to SMSI effects. The maximum cobalt loading achievable in a single impregnation was 6 wt.% by using crystalline niobia as support. A decrease in activity per unit weight of cobalt was observed by increasing the cobalt loading using multiple impregnations, due to formation of larger cobalt particles and decreased interaction of cobalt with the

support. Additionally, this decreased cobalt-support interaction suppressed the beneficial effect of niobia on C_{5+} selectivity. A facile carbon deposition method was used to restrict the collapse of the niobium oxide hydrate porous structure during crystallization. The carbon on the surface acted as structural template at the high temperatures needed to obtain crystalline niobia. The resulting crystalline niobia displayed an important fraction of the mesopores from the niobium oxide hydrate. The porous niobia was used as support to prepare cobalt catalysts and further tested in industrially relevant conditions for the Fischer–Tropsch synthesis. These catalysts proved to be highly active and selective. The porous structure allowed higher cobalt loadings leading to an increased weight-normalized catalytic activity. Furthermore, this porosity prevented the cobalt particles from sintering, resulting in very stable catalysts. STEM-EDX mapping characterization made possible to determine cobalt particle size and distribution in the catalysts, this technique demonstrated to be a powerful tool to study systems where phase distinction between its components is difficult due to similar electron density.

Appendix A. Supplementary data

Supplementary data associated with this article can be found, in the online version, at http://dx.doi.org/10.1016/j.apcata.2017.07.016.

References

[1] A.Y. Khodakov, W. Chu, P. Fongarland, Chem. Rev. 107 (2007) 1692–1744.
[2] R.R. Soares, A. Frydman, M. Schmal, Catal. Today 16 (1993) 361–370.
[3] R.R.C.M. Silva, M. Schmal, R. Frety, J.A. Dalmon, Chem. Soc. Faraday Trans. 89 (1993) 3975–3980.
[4] A. Frydman, R.R. Soares, M. Schmal, Proceedings of the 10th International Congress on Catalysis (1993) 2797–2800.
[5] J.H. den Otter, K.P. de Jong, Top. Catal. 57 (2013) 445–450.
[6] J.H. den Otter, S.R. Nijveld, K.P. de Jong, ACS Catal. 6 (2016) 1616–1623.
[7] J.H. den Otter, H. Yoshida, C. Ledesma, D. Chen, K.P. de Jong, J. Catal. 340 (2016) 270–275.
[8] J.H. den Otter, PhD thesis, Niobia-supported Cobalt Catalysts for Fischer-Tropsch Synthesis, Utrecht University, 2016, 2016.

[9] I. Nowak, M. Ziolek, Chem. Rev. 99 (1999) 3603–3624.

[10] X. Chen, T. Yu, X. Fan, H. Zhang, Z. Li, J. Ye, Z. Zou, Appl. Surf. Sci. 253 (2007) 8500–8506.

[11] S. Kim, I. Jeong, J. Hwang, M.J. Ko, J. Lee, Chem. Commun. (2017), http://dx.doi.org/10.1039/C7CC01400G.

[12] B. Lee, D. Lu, J.N. Kondo, K.J. Domen, J. Am. Chem. Soc. 124 (2002) 11256–11257.

[13] E.R. Leite, C. Vila, J. Bettini, E. Longo, J. Phys. Chem. B 110 (2006) 18088–18090.

[14] T. Murayama, J. Chen, J. Hirata, K. Matsumoto, W. Ueda, Catal. Sci. Technol. 4 (2014) 4250–4257.

[15] E.R. Leite, C. Vila, J. Bettini, E. Longo, J. Phys. Chem. B 110 (2006) 18088–18090.

[16] S. Chai, H.P. Wang, Y. Liang, B.Q. Xu, J. Catal. 250 (2007) 342–349.

[17] L.K. Frevel, H.W. Rinn, Anal. Chem. 27 (1955) 1329–1330.

[18] H. Schäfer, R. Gruehn, F. Schulte, Angew. Chem. Int. Ed. 5 (1966) 40–52.

[19] F.B. Noronha, C.A. Perez, R. Frety, Phys. Chem. Chem. Phys. 1 (1999) 2861–2867.

[20] B. Sexton, J. Catal. 97 (1986) 390–406.

[21] G. Jacobs, Y. Ji, B.H. Davis, D. Cronauer, A.J. Kropf, C.L. Marshall, Appl. Catal. A 333 (2007) 177–191.

[22] J.P. den Breejen, A.M. Frey, J. Yang, A. Holmen, M.M. Schooneveld, F.M.F. Groot, O. Stephan, J.H. Bitter, K.P. de Jong, Top. Catal. 54 (2011) 768–777.